Biophysical Chemistry 157 (2011) 33–42

Contents lists available at ScienceDirect

Biophysical Chemistry

journal homepage: http://www.elsevier.com/locate/biophyschem

A theoretical modeling for frequency modulation of Ca^{2+} signal on activation of MAPK cascade

Ming Yi [a,*,1], Qi Zhao [a,b,1], Jun Tang [c], Canjun Wang [d]

[a] Wuhan Institute of Physics and Mathematics, Chinese Academy of Sciences, Wuhan 430071, China
[b] Graduate University of Chinese Academy of Sciences, Beijing 100049, China
[c] College of Science, China University of Mining and Technology, Xuzhou 221008, China
[d] Nonlinear Research Institute, Baoji University of Arts and Sciences, Baoji 721007, China

ARTICLE INFO

Article history:
Received 13 January 2011
Received in revised form 4 April 2011
Accepted 7 April 2011
Available online 13 April 2011

Keywords:
Ca^{2+} oscillations
GTPase-cycle
MAPK cascade
Integrated theoretical models
Frequency modulation
Negative correlation

ABSTRACT

It is known that Ca^{2+} signal regulates mitogen-activated protein kinase (MAPK) cascade by a central Ras protein in GTPase-cycle. Therefore, we construct an integrated theoretical model comprising Ca^{2+} oscillations, GTPase-cycle and MAPK cascade modules sequentially. Meanwhile, based on multiple feedback regulations in MAPK cascade, three operation modes of this model are introduced. An extended version of this model is further built when spatial heterogeneity is involved. These models allow us to investigate the very interesting and broad question about the effects of Ca^{2+} oscillations on the activation of MAPK cascade in both the homogeneous and heterogeneous systems. When the Li–Rinzel model is adopted to simulate endogenous Ca^{2+} oscillations, our theoretical results illustrate that the appropriate operation mode of MAPK cascade is required for the negative correlation between a decreasing frequency of Ca^{2+} oscillations and activation of MAPK cascade, which was found in the experiment (S. Kupzig et al. PNAS 102 (2005) 7577–7582). While a piecewise function is used to generate Ca^{2+} signal to explore much larger range of periods of Ca^{2+} oscillations, it is found that the negative correlation feature is independent on the operation mode of MAPK cascade. In this case, different operation modes only influence the strength of negative correlation between activation of MAPK cascade and periods of Ca^{2+} oscillations. The quantitative results may be of great use in analyzing interaction of IP3 — Ca^{2+} and Ras–MAPK signaling pathways, and motivate the further experimental research.

1. Introduction

It is well known that, many cell-surface receptors, such as G-protein coupled receptors (GPCRs), receptor tyrosine kinases (RTKs) and cytokine receptors, receive environmental stimulus. These extracellular signals activate different signaling transduction pathways. As the central integration modules for cellular information processing, signaling pathways play pivotal roles in the control of fundamental cellular processes that include cell growth and division, migration, and differentiation [1,2]. To get a better understanding of signaling pathways in cellular processes, the experimental and theoretical studies are required.

Ca^{2+} signal plays important roles in biological functions. Almost everything we do is controlled by Ca^{2+}, for example, how we move, how our heart beats, and how our brain processes and stores information [3,4]. Ca^{2+} acts as an intracellular messenger, carrying information within cells and regulating their activities. It serves for various purposes, such as triggering life at fertilization, controlling the development and differentiation of cells into specialized types, mediating neural activity, and learning or inducing cell death. In this respect, we call it a second messenger. It is natural that much effort has been devoted to understand the functional role of Ca^{2+}[5,6]. Some experiments found that Ca^{2+} signal encodes extracellular information and guides further appropriate response via oscillation amplitude, duration, frequency and spatial patterning [7,8].

Increased cytosolic Ca^{2+} concentrations initiate the activation of several kinase-dependent signaling cascades. Multiple target proteins are modulated by intracellular Ca^{2+} oscillations [9–11]. The information encoded in Ca^{2+} oscillations is decoded by these downstream signal proteins. It is known that MAPK cascade plays vital roles on the decoding of Ca^{2+} oscillations. A MAPK cascade consists of three sequentially acting kinases, comprising MAPK, MAPK kinase (MAP2K) and MAP2K kinase (MAP3K). Each kinase, if activated, can activate its downstream substrate by phosphorylation reactions. The active kinase can be deactivated by dephosphorylation reactions. Through MAPK cascade, the external signals can be propagated from the cell membrane to nucleus [12–17]. The biological outcome of stimulation depends on the temporal profile of active, bisphosphorylated MAPK (ppMAPK) in the perinuclear area [18].

* Corresponding author.
E-mail address: yiming@wipm.ac.cn (M. Yi).
[1] These authors contributed equally to this work.

0301-4622/$ – see front matter © 2011 Elsevier B.V. All rights reserved.
doi:10.1016/j.bpc.2011.04.007

The coupling between Ca^{2+} oscillations and MAPK cascade is explored extensively by experimental researches. It appears that Ras kinase in the GTPase-cycle combines Ca^{2+} signal with MAPK cascade [19–21]. An example of a potential link between Ca^{2+} and MAPK is that, in the brain, Ca^{2+} is fundamental in the control of synaptic activity and memory formation [22]. Synaptic activity results in the elevation of cytosolic Ca^{2+} levels. Increased cytosolic Ca^{2+} concentrations initiate the activation of MAPK cascade, leading to CREB activation and phosphorylation at Ser133, a process critical for protein synthesis-dependent synaptic plasticity and LTP [23,24]. Especially, Kupzig et al. have examined experimentally the roles of frequencies of Ca^{2+} oscillations on activation of Ras and the ERK/MAPK cascade [25]. Two observations were provided in the experiment. First, a non-linear increase in Ras-GTP (also ppMAPK) was observed with increasing Ca^{2+} oscillatory frequency, i.e., there exists a negative correlation between Ras-GTP (also ppMAPK) and the period of Ca^{2+} oscillations. Second, oscillatory Ca^{2+} signal reduces the effective Ca^{2+} threshold for the activation of Ras compared with the constant Ca^{2+} signal.

With the increase of experimental data and information, it is now possible to study Ca^{2+}-mediated MAPK signaling pathway quantitatively at a system level. The previous experimental researches advance our knowledge about the roles of Ca^{2+} oscillations on MAPK cascade, however, the related theoretical researches are still rare. Diaz et al. have built a theoretical model including the interaction of Ca^{2+} signaling system with MAPK cascade during the FGF mesodermal induction process [26]. But in their model, Ca^{2+} signal is coupled with MAPK cascade by PKC-mediated activation of MAP3K. Zhao et al. have established a combined model in which a minimal Li–Rinzel model for Ca^{2+} signal is coupled with a phosphorylation–dephosphorylation cycle model [27]. However, they only investigated the information transmission from IP_3 to target protein.

Motivated by the experimental work [25], some further considerations about Ca^{2+}-mediated MAPK signaling pathway are presented. In order to predict the modulation properties of Ca^{2+} oscillations on MAPK cascade, one way would be to use computer simulations [19]. Therefore, we attempt to investigate the underlying mechanisms for experimental observations by theoretical modeling. It is also noticed that there exist multiple feedback regulations in MAPK cascade. But how these possible feedbacks affect the roles of Ca^{2+} oscillations on MAPK cascade is unclear. In addition, the kinase proteins are localized spatially. Hence, another interesting problem is how Ca^{2+} oscillations regulates MAPK cascade when these spatial effects are considered. To the best knowledge of ours, these problems have not been studied so far.

Therefore, to address the above problems, this paper is organized as below. First, in Section 2, we develop an integrated theoretical model for Ca^{2+}-mediated MAPK signaling pathway in the homogeneous system. Especially, based on different types of feedback in MAPK cascade, three operation modes are introduced. Next, an extended theoretical model, i.e., a reaction-diffusion model is built when the spatial effects are involved in the heterogeneous system. Furthermore, in Section 3, using our models, we identify how the average Ras-GTP concentration depends on the periods of Ca^{2+} oscillations when the Li–Rinzel model is adopted to generate Ca^{2+} oscillations. Then we compare the difference between an oscillatory Ca^{2+} signal and a constant one on activation of Ras-GTP. Also, for different modes, we investigate systematically the frequency modulations of Ca^{2+} signal on activation of MAPK cascade under both the homogeneous and heterogeneous systems when Ca^{2+} signal is generated by the Li–Rinzel model or a piecewise function. Finally, in Section 4, we end with our conclusions and discussions.

2. Models

To investigate the regulation properties of Ca^{2+} oscillations on MAPK cascade, we need to employ theoretical modeling for Ca^{2+}-mediated MAPK signaling pathway. This pathway consists of three modules, i.e., Ca^{2+} oscillations, GTPase-cycle and MAPK cascade. A schematic of network structures for this signaling pathway is shown in Fig. 1. Below, the mathematical models of three modules are introduced, respectively. Then we construct two integrated models about this signaling pathway by integrating these three modules under the homogeneous and heterogeneous conditions.

2.1. Ca^{2+} oscillation module

We use the minimal two-variable Li–Rinzel model to mimic endogenous Ca^{2+} oscillations in cytoplasm [28]. The variables of Li–Rinzel model used are the free cytosolic Ca^{2+} concentration (C) and the fraction of open IP_3 receptor subunits (h), whose dynamical behaviors are controlled by the following rate equations,

$$\frac{dC}{dt} = J_{chan}(C,I) + J_{leak}(C) - J_{pump}(C), \tag{1}$$

$$\frac{dh}{dt} = \frac{h_\infty - h}{\tau_h}. \tag{2}$$

The dynamics of C is controlled by the three fluxes: (i) a Ca^{2+} release (J_{chan}), which is gated by Ca^{2+} and IP_3 concentration (I), (ii) a passive leak of Ca^{2+} from the endoplasmic reticulum (ER) to cytosol (J_{leak}), and (iii) an active uptake of Ca^{2+} into ER (J_{pump}) due to the action pumps. These fluxes can be expressed as

$$J_{chan}(C,I) = u_1 m_\infty^3 h^3 [C_0 - (1+c_1)C],$$
$$J_{leak}(C) = u_2 [C_0 - (1+c_1)C],$$
$$J_{pump}(C) = \frac{u_3 C^2}{K_3^2 + C^2}.$$

The gating variables and their time scales are given by $m_\infty = \frac{I}{I+d_1}\frac{C}{C+d_5}$, $h_\infty = \frac{Q_2}{Q_2+C}$, and $\tau_h = \frac{1}{a_2(Q_2+C)}$ with $Q_2 = \frac{I+d_1}{I+d_3}d_2$. For more details about the two-variable LR model, see Ref. [28]. The parameter values we use are $u_1 = 6\ s^{-1}$, $u_2 = 0.11\ s^{-1}$,

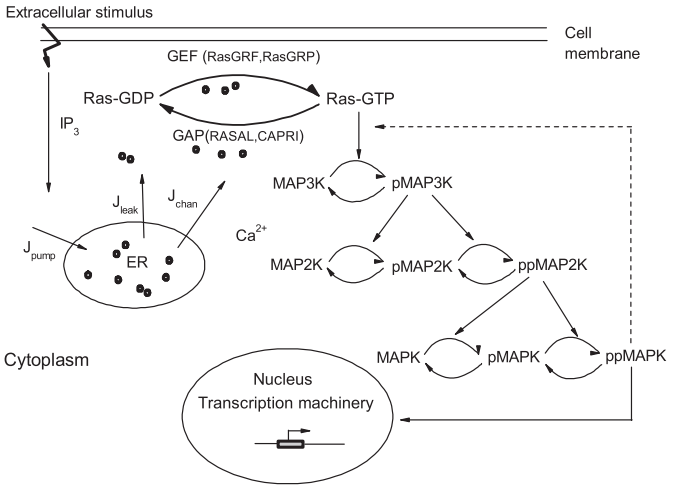

Fig. 1. Schematic of network structures for Ca^{2+}-modulated MAPK cascade signaling pathway. Ca^{2+} signal, released from internal Ca^{2+} store (i.e., ER), regulates Ras activation. MAP3K is initially activated by Ras-GTP and becomes phosphorylated MAP3K (i.e. pMAP3K). Then pMAP3K activates MAP2K, and bisphosphorylated MAP2K (i.e., ppMAP2K) further phosphorylates MAPK. The coupling between Ca^{2+} oscillations module and MAPK cascade module is considered by Ca^{2+}-mediated activation of Ras in the GTPase-cycle module. The exchange between GTP and GDP is controlled by two antagonistic proteins, i.e., GEF and GAP.

$u_3 = 0.9\ s^{-1}$, $C_0 = 2\ \mu M$, $c_1 = 0.185$, $K_3 = 0.051\ \mu M$, $d_1 = 0.13\ \mu M$, $d_2 = 1.049\ \mu M$, $d_3 = 0.9434\ \mu M$, $d_5 = 0.08234\ \mu M$, and $a_2 = 0.2\ \mu M^{-1}s^{-1}$.

Previous researches indicated that Ca^{2+} signal can encode information via frequency-modulation or amplitude-modulation in response to external stimulus [29,30]. Kupzig et al. used the oscillatory Ca^{2+} signal with fixed amplitude while the period was changed in their experiment [25]. Hence, we focus on the frequency-modulation of Ca^{2+} oscillations. When $K_3 = 0.051$, with increasing the intensity of IP_3, it is observed that the amplitude is nearly unchanged (see Fig. 2(a)) while the frequency of Ca^{2+} oscillations is increased (see Fig. 2(b)). In our work, we let IP_3 vary from 0.85 to 0.55 μM, the period changes from 18.33 to 31.55 s correspondingly.

2.2. GTPase-cycle module

Ca^{2+} oscillation is coupled with MAPK cascade by a key protein (i.e., Ras) in the GTPase-cycle, as shown in Fig. 1. Ras represents one superfamily of small GTPases, which function as a molecular switch by cycling between an inactive GDP-bound state (Ras–GDP) and an active GTP-bound state (Ras–GTP). This process is facilitated by guanine nucleotide exchange factor (GEF) for activation and GTPase-activating protein (GAP) for inhibition of Ras.

Increased cytosolic Ca^{2+} regulates two families of GEF kinase (including Ras–GRF and Ras–GRP). Ras–GRF associates with Ca^{2+}/calmodulin indirectly, whereas a more direct control is achieved through association of Ca^{2+} with a typical EF hands for Ras–GRP. The binding of Ca^{2+} to GEF protein activates GEF (the active form is denoted by GEF*). For simplicity, Ras–GRF and Ras–GRP are integrated into one variable. We use the mass action rule to describe this binding process of Ca^{2+}, i.e., the activation rate of the enzyme (GEF*) is assumed to be linear with respect to the Ca^{2+} and the GFF concentration. In addition, there is a first-order degradation in the GEF* concentration. Therefore, the evolution for GEF* is governed by the following equations

$$\frac{d[GEF^*]}{dt} = k_1([GEF]_{tot} - [GEF^*])C^n - k_2[GEF], \tag{3}$$

$$[GEF]_{tot} = [GEF] + [GEF^*]. \tag{4}$$

Analogously, the evolution equations for GAP* are written as

$$\frac{d[GAP^*]}{dt} = k_3([GAP]_{tot} - [GAP^*])C^n - k_4[GAP^*], \tag{5}$$

$$[GAP]_{tot} = [GAP] + [GAP^*]. \tag{6}$$

Where $[GEF]_{tot}$ and $[GAP]_{tot}$ are the total concentrations of GEF and GAP, n describes how GEF and GAP are activated cooperatively by Ca^{2+}.

Because the binding and unbinding rates are much faster than the changes in the GAP* and GEF* concentrations, one can use the quasi-steady-state approximation with respect to the GEF* and GAP* level, respectively. Thus, we obtain $[GEF^*] = \frac{k_1 C^n [GEF]_{tot}}{k_1 C^n + k_2}$ and $[GAP^*] = \frac{k_3 C^n [GAP]_{tot}}{k_3 C^n + k_4}$.

Furthermore, we use the mass action rule to describe activation and deactivation reactions of Ras. The GTPase-cycle is governed by the following equation

$$\frac{d[Ras-GTP]}{dt} = k_{on}([Ras]_{tot} - [Ras-GTP])[GEF^*] - k_{off}[Ras-GTP][GAP^*]. \tag{7}$$

Where k_{on} and k_{off} denote the activation and deactivation rates of Ras in the GTPase-cycle module, respectively. Based on the expressions of GEF* and GAP*, consequently, Eq. (7) becomes

$$\frac{d[Ras-GTP]}{dt} = k_{on}([Ras]_{tot} - [Ras-GTP])\frac{C^n[GEF]_{tot}}{C^n + \frac{k_2}{k_1}} - k_{off}[Ras-GTP]\frac{C^n[GAP]_{tot}}{C^n + \frac{k_4}{k_3}}. \tag{8}$$

Some simplifications for Ras-GTP are adopted. Two effective reaction rates, including $k_{32} = k_{on}[GEF]_{tot}$ (effective activation rate) and $k_{34} = k_{off}[GAP]_{tot}$ (effective deactivation rate), are provided to obtain compact expressions. In order to describe Ca^{2+}-mediated activation of Ras with classical Michaelis–Menten kinetics (i.e., a normal Hill function), $\frac{k_2}{k_1}$ is replaced by k_{33}^n and $\frac{k_4}{k_3}$ is replaced by k_{35}^n. Based on these assumptions, we further obtain

$$\frac{d[Ras-GTP]}{dt} = \frac{k_{32}C^n}{k_{33}^n + C^n}([Ras]_{tot} - [Ras-GTP]) - \frac{k_{34}C^n}{k_{35}^n + C^n}[Ras-GTP]. \tag{9}$$

Furthermore, the Ras is deactivated due to the binding of GAP (including CAPRI and RASAL) with cell membrane. An elevation in Ca^{2+} only can induce a transient association of CAPRI or oscillatory association of RASAL with cell membrane. Therefore, in most time, the GAP concentration in cell membrane is low. For convenience, we assume that Ca^{2+} concentration is higher than GAP level near the cell membrane so that the deactivation rate of Ras is independent of GAP. Such treatment also reduces the number of unknown parameters. Besides the Ca^{2+}-dependent activation of Ras, Ras-GTP can also be

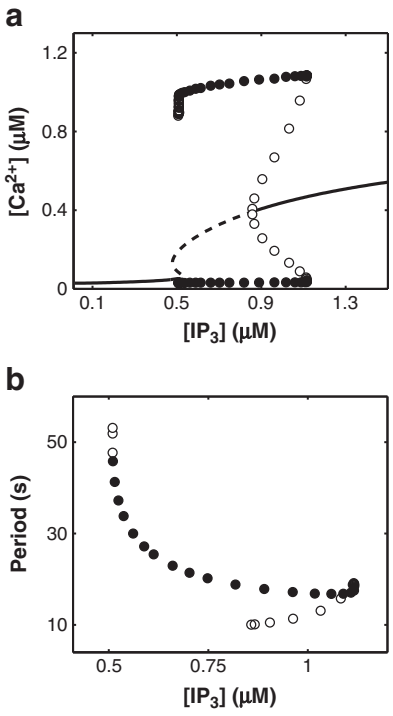

Fig. 2. (a) Bifurcation diagram and (b) period diagram of the Li-Rinzel model with $K_3 = 0.051\ \mu M$. Stable fixed points (—), unstable ones (— — —), stable limit cycles (•), unstable ones (◦).

produced by Ca^{2+}-independent activation with a small basal production rate, such as through receptor-activated Grb-SOS pathway. Hence, a basal activation rate of Ras (i.e., k_{31}) is added. Finally, a reduced model for GTPase-cycle module is derived as below

$$\frac{d[Ras{-}GTP]}{dt} = \left(k_{31} + \frac{k_{32}C^n}{k_{33}^n + C^n}\right)([Ras]_{tot} - [Ras{-}GTP]) - k_{34}[Ras{-}GTP]. \tag{10}$$

The parameter values are $k_{31} = 0.001\ s^{-1}$, $k_{32} = 2.0\ s^{-1}$, $k_{33} = 1.0\ \mu M$, and $k_{34} = 0.6\ s^{-1}$.

2.3. MAPK cascade module

2.3.1. MAPK cascade under the homogeneous case

As described in Fig. 1, a three-layer MAPK cascade, consisting of MAP3K, MAP2K and MAPK, is adopted. MAP3K is initially activated by Ras-GTP and becomes phosphorylated MAP3K (i.e. pMAP3K). Then pMAP3K activates MAP2K by phosphorylating its two residues sequentially. Bisphosphorylated MAP2K (i.e., ppMAP2K) also phosphorylates MAPK on two conserved threonine and tyrosine residues. It is in this stage bisphosphorylated MAPK (i.e., ppMAPK) is generated. For the homogenous (well-stirred) system, the rate equations are employed to describe this MAPK signaling pathway. We consider a similar model to the one developed by Huang et al. [31], but different types of feedback are involved in our model. The rate equations which describe the homogeneous system are

$$\frac{d[pMAP3K]}{dt} = v_1 - v_2, \tag{11}$$

$$\frac{d[pMAP2K]}{dt} = v_3 - v_4 + v_5 - v_6, \tag{12}$$

$$\frac{d[ppMAP2K]}{dt} = v_4 - v_5, \tag{13}$$

$$\frac{d[pMAPK]}{dt} = v_7 - v_8 + v_9 - v_{10}, \tag{14}$$

$$\frac{d[ppMAPK]}{dt} = v_8 - v_9. \tag{15}$$

Phosphorylation and dephosphorylation rates for these equations are derived from Michaelis–Menten kinetics, their expressions are given in Table 1.

The values of parameters are listed in Table 2. For further details about the definitions and estimations of the parameters, see Refs. [32,33]. F_a corresponds to the strength of positive feedback, while F'_a corresponds to the strength of negative feedback, which are estimated empirically. k_1^{cat}, k_3^{cat}, k_4^{cat}, k_7^{cat} and k_8^{cat} are catalytic rate constants. V_{max2}, V_{max5}^m, V_{max6}^m, V_{max5}^c, V_{max6}^c, V_{max9} and V_{max10} are maximal enzyme rates. K_a, K_{m1}, K_{m2}, K_{m3}, K_{m4}, K_{m5}^m, K_{m6}^m, K_{m5}^c, K_{m6}^c, K_{m7}, K_{m8}, K_{m9} and K_{m10} are Michaelis constants. V_{max5}^m, V_{max6}^m, K_{m4} and K_{m5}^m are the rates which describe the reactions occur at cell membrane, while V_{max5}^c, V_{max6}^c, K_{m5}^c and K_{m6}^c correspond to the reactions occur in the cytoplasm.

Although the basic structure of all MAPK cascades is the same in a variety of cells, MAPK cascades are tightly controlled by different types of feedback. For instance, the basic feature of MAPK cascade with no feedback for the sensitivity amplification is known as ultrasensitivity [31,34–36], which means steeply sigmoidal responses of ppMAPK to the change of input signal. Furthermore, a positive or negative feedback from downstream kinase (MAPK) to the top of the cascade (MAP3K) is also found to exist in the MAPK cascade [32,33,37,38]. We use to Eqs. (11)–(15) to investigate steady state dependence of ppMAPK on Ras-GTP for different feedback control in Fig. 3. Based on different responses, we define three operation modes for our MAPK cascade.

- Operation mode I
  There is no feedback of ppMAPK on upstream protein in this mode, which leads to ultrasensitivity responses for the whole cascade (Fig. 3(a)). Here the parameters are chosen as $F_a = 1$ and $F'_a = 1$.
- Operation mode II
  There exists a positive feedback in which MAPK positively controls the rate of MAP3K phosphorylation, resulting in bistability for the whole cascade (Fig. 3(b)). We only let $F_a = 5$ and $F'_a = 1$.
- Operation mode III
  There is a negative feedback in which MAPK negatively controls the rate of MAP3K phosphorylation, leading to a limit cycle oscillation of ppMAPK (Fig. 3(c)). We use $F_a = 1$ and $F'_a = 5$ in this case.

For these operation modes, an interesting problem is which mode is preferential for biological species. Owing to biological diversity, different cells perhaps select different feedback and regulatory mechanisms. Therefore, the regulation properties of Ca^{2+} oscillations on MAPK cascade under three operation modes are explored in the following sections.

Table 1
Kinetic description of the MAPK cascade reactions for the homogeneous system.

Reaction	Rate
$MAP3K \rightarrow pMAP3K$	$v_1 = \frac{k_1^{cat}[Ras{-}GTP][MAP3K]}{(K_{m1} + [MAP3K])} \frac{\left(1 + F_a([ppMAPK]/K_a)^2\right)}{\left(1 + F'_a([ppMAPK]/K_a)^2\right)}$
$pMAP3K \rightarrow MAP3K$	$v_2 = \frac{V_{max2}[pMAP3K]}{(K_{m2} + [pMAP3K])}$
$MAP2K \rightarrow pMAP2K$	$v_3 = \frac{k_3^{cat}[pMAP3K][MAP2K]}{(K_{m3} + [MAP2K])}$
$pMAP2K \rightarrow ppMAP2K$	$v_4 = \frac{k_4^{cat}[pMAP3K][pMAP2K]}{(K_{m4} + [pMAP2K])}$
$ppMAP2K \rightarrow pMAP2K$	$v_5 = \frac{V_{max5}^c[ppMAP2K]}{(K_{m5}^c + [ppMAP2K])}$
$pMAP2K \rightarrow MAP2K$	$v_6 = \frac{V_{max6}^c[pMAP2K]}{(K_{m6}^c + [pMAP2K])}$
$MAPK \rightarrow pMAPK$	$v_7 = \frac{k_7^{cat}[ppMAP2K][MAPK]}{(K_{m7} + [MAPK])}$
$pMAPK \rightarrow ppMAPK$	$v_8 = \frac{k_8^{cat}[ppMAP2K][pMAPK]}{(K_{m8} + [pMAPK])}$
$ppMAPK \rightarrow pMAPK$	$v_9 = \frac{V_{max9}[ppMAPK]}{(K_{m9} + [ppMAPK])}$
$pMAPK \rightarrow MAPK$	$v_{10} = \frac{V_{max10}[pMAPK]}{(K_{m10} + [pMAPK])}$

Table 2
Model parameters in MAPK cascade module.

Parameter	Value	Parameter	Value
k_1^{cat}	$0.2\ s^{-1}$	K_{m1}	50 nM
K_a	100 nM	V_{max2}	$5\ nMs^{-1}$
K_{m2}	50 nM	k_3^{cat}	$1\ s^{-1}$
K_{m3}	130 nM	k_4^{cat}	$5\ s^{-1}$
K_{m4}	50 nM	V_{max5}^m	$100\ nMs^{-1}$
K_{m5}^m	100 nM	V_{max6}^m	$100\ nMs^{-1}$
K_{m6}^m	100 nM	V_{max5}^c	$100\ nMs^{-1}$
K_{m5}^c	100 nM	V_{max6}^c	$100\ nMs^{-1}$
K_{m6}^c	100 nM	k_7^{cat}	$1\ s^{-1}$
K_{m7}	50 nM	k_8^{cat}	$20\ s^{-1}$
K_{m8}	50 nM	V_{max9}	$380\ nMs^{-1}$
K_{m9}	10 nM	V_{max10}	$50\ nMs^{-1}$
K_{m10}	18 nM	$[MAPK]_{tot}$	360 nM
$[MAP2K]_{tot}$	200 nM	$[MAP3K]_{tot}$	200 nM
$[Ras]_{tot}$	100 nM		

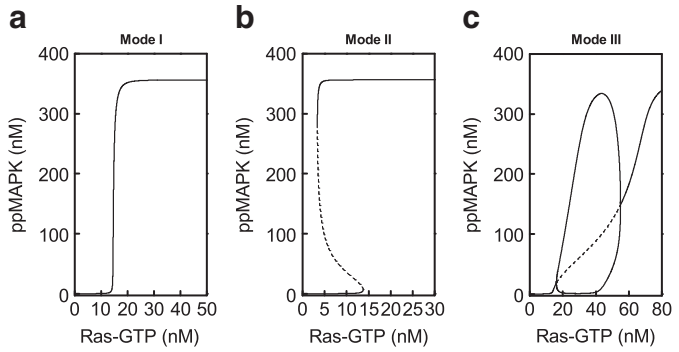

Fig. 3. Steady state dependence of ppMAPK on Ras-GTP for three operation modes, steady state (−), unstable state (− − −).

2.3.2. MAPK cascade under the heterogeneous case

Above, we have constructed a theoretical model in the well-stirred case. However, under real biological conditions, the spatial effects cannot be neglected [14–17,33,39]. First, in the MAPK cascade, the kinase proteins are localized in different space so that the cascade is activated spatially. MAPK is phosphorylated and dephosphorylated in the cytoplasm, while MAP3K is phosphorylated and dephosphorylated at the cell membrane. Especially, MAP2K is phosphorylated by pMAP3K close to the cell membrane while it is dephosphorylated in the cytoplasm, which shows spatial separation of two antagonistic regulatory proteins. Second, the stimulus signal from extracellular ligands must propagate into nucleus by diffusion. The spatial diffusion of activated kinases is crucial for signal propagation. So, these spatial factors should be taken into account. To extend the above theoretical model in the homogeneous case, a reaction-diffusion model in the heterogeneous case is constructed.

The reaction-diffusion model for one-dimensional spatial domain is formulated as follows:

$$\frac{d[pMAP3K]}{dt} = v_1^m - v_2^m, \tag{16}$$

$$\frac{\partial[pMAP2K]}{\partial t} = \left(\frac{D}{R^2}\right)\frac{1}{x^2}\frac{\partial}{\partial x}\left(x^2\frac{\partial[pMAP2K]}{\partial x}\right) + v_5^c - v_6^c, \tag{17}$$

$$\frac{\partial[ppMAP2K]}{\partial t} = \left(\frac{D}{R^2}\right)\frac{1}{x^2}\frac{\partial}{\partial x}\left(x^2\frac{\partial[ppMAP2K]}{\partial x}\right) - v_5^c, \tag{18}$$

$$\frac{\partial[pMAPK]}{\partial t} = \left(\frac{D}{R^2}\right)\frac{1}{x^2}\frac{\partial}{\partial x}\left(x^2\frac{\partial[pMAPK]}{\partial x}\right) + v_7^c - v_8^c + v_9^c - v_{10}^c, \tag{19}$$

$$\frac{\partial[ppMAPK]}{\partial t} = \left(\frac{D}{R^2}\right)\frac{1}{x^2}\frac{\partial}{\partial x}\left(x^2\frac{\partial[ppMAPK]}{\partial x}\right) + v_8^c - v_9^c. \tag{20}$$

The boundary conditions for protein components in Eqs. (16)–(20) are set as follows:

$$\frac{\partial[pMAP2K]}{\partial x}|_{x=R} = \frac{R^2}{3D}(v_3^m - v_4^m + v_5^m - v_6^m), \tag{21}$$

$$\frac{\partial[ppMAP2K]}{\partial x}|_{x=R} = \frac{R^2}{3D}(v_4^m - v_5^m), \tag{22}$$

$$\frac{\partial[pMAP2K]}{\partial x}|_{x=r} = \frac{\partial[ppMAP2K]}{\partial x}|_{x=r} = 0, \tag{23}$$

$$\frac{\partial[pMAPK]}{\partial x}|_{x=R} = \frac{\partial[pMAPK]}{\partial x}|_{x=r} = 0, \tag{24}$$

Table 3
Kinetic description of the MAPK cascade reactions that occur at cell membrane for our heterogeneous system.

Reaction	Rate
$MAP3K \rightarrow pMAP3K$	$v_1^m = \frac{k_1^{cat}[Ras-GTP][MAP3K]}{(K_{m1}+[MAP3K])}\frac{\left(1+F_a([ppMAPK]/K_a)^2\right)}{\left(1+F_a'([ppMAPK]/K_a)^2\right)}$
$pMAP3K \rightarrow MAP3K$	$v_2^m = \frac{V_{max2}[pMAP3K]}{(K_{m2}+[pMAP3K])}$
$MAP2K \rightarrow pMAP2K$	$v_3^m = \frac{k_3^{cat}[pMAP3K][MAP2K]}{(K_{m3}+[MAP2K])}$
$pMAP2K \rightarrow ppMAP2K$	$v_4^m = \frac{k_4^{cat}[pMAP3K][pMAP2K]}{(K_{m4}+[pMAP2K])}$
$ppMAP2K \rightarrow pMAP2K$	$v_5^m = \frac{V_{max5}^m[ppMAP2K]}{(K_{m5}^m+[ppMAP2K])}$
$pMAP2K \rightarrow MAP2K$	$v_6^m = \frac{V_{max6}^m[pMAP2K]}{(K_{m6}^m+[pMAP2K]}$

The rate expressions are given in Tables 3 and 4. For the corresponding three operation modes in our heterogeneous system, the same parameter values are used. We just consider Eqs. (16)–(25) in a volume between two concentric spheres, corresponding to cell and nuclear membrane. Cell radius is denoted by R while nuclear radius is r. We fix cell radius $R=15\,\mu m$, nuclear radius $r=6\,\mu m$, it means the propagation length $L=R-r=9\,\mu m$ while the spherical symmetry is used so that we can make the analysis of signaling in three dimensions nearly equivalent to the analysis in one dimension. Numerical methods are also provided in Supplementary Material. The diffusion coefficient D in the cytoplasm was reported to be in a range of 1–10 $\mu m^2 s^{-1}$[40]. We assume $D=5\,\mu m^2 s^{-1}$ for all active kinase proteins.

2.4. Integrated theoretical models of Ca^{2+}-mediated MAPK signaling pathway

We attempt to study the frequency modulations of Ca^{2+} signal on activation of MAPK cascade under both the homogeneous and heterogeneous cases. Therefore, two integrated theoretical models of Ca^{2+}-mediated MAPK signaling pathway are built, respectively.

The integrated theoretical model in the homogeneous case (denoted by HOC model) is obtained by combining three modules, including Ca^{2+} oscillations (Eqs. (1) and (2)), GTPase-cycle (Eq. (10))

Table 4
Kinetic description of the MAPK cascade reactions in the cytoplasm for our heterogeneous system.

Reaction	Rate
$ppMAP2K \rightarrow pMAP2K$	$v_5^c = \frac{V_{max5}^c[ppMAP2K]}{(K_{m5}^c+[ppMAP2K]}$
$pMAP2K \rightarrow MAP2K$	$v_6^c = \frac{V_{max6}^c[pMAP2K]}{(K_{m6}^c+[pMAP2K]}$
$MAPK \rightarrow pMAPK$	$v_7^c = \frac{k_7^{cat}[ppMAP2K][MAPK]}{(K_{m7}+[MAPK])}$
$pMAPK \rightarrow ppMAPK$	$v_8^c = \frac{k_8^{cat}[ppMAP2K][pMAPK]}{(K_{m8}+[pMAPK])}$
$ppMAPK \rightarrow pMAPK$	$v_9^c = \frac{V_{max9}[ppMAPK]}{(K_{m9}+[ppMAPK])}$
$pMAPK \rightarrow MAPK$	$v_{10}^c = \frac{V_{max10}[pMAPK]}{(K_{m10}+[pMAPK])}$

and MAPK cascade (Eqs. (11)–(15)) while the integrated theoretical model in the heterogeneous case (denoted by HEC model) is derived by linking Ca^{2+} oscillations (Eqs. (1) and (2)), GTPase-cycle (Eq. (10)) with MAPK cascade (Eqs. (16)-(25)). It is obvious that the HEC model is just an extended version of the HOC model when the spatial heterogeneity is included. Here we should notice, although Eqs. (1) and (2) and (10) describe a homogeneous Ca^{2+} and Ras-GTP density, we can still use these equations to represent Ca^{2+} and Ras-GTP concentrations close to cell membrane in HEC model.

3. Results

3.1. Negative correlation between Ras-GTP and period of Ca^{2+} signal

With increasing the period of Ca^{2+} oscillations, a nonlinear decrease of activation of Ras was uncovered (see Fig. 3(a) in Ref. [25]), which implied a negative correlation between the activation of Ras and period of Ca^{2+} oscillations. It is an interesting phenomenon. Salazar et al. pointed out that the average is a good measure of target protein's response if the amplitude of protein activity oscillations is not too large, even if the target amplitudes are large, the average is useful diagnostic of how sensitively the system responds to the oscillatory signal [41]. Thus, we use the average Ras-GTP concentration as the response of active Ras.

By virtue of the theoretical model including Ca^{2+} oscillations module (Eqs. (1) and (2)) and GTPase-cycle module (Eq. (10)), the dependence of average Ras-GTP on the period of Ca^{2+} oscillations is plotted in Fig. 4(a). The average level of Ras-GTP exhibits a monotonically decreasing dependence on the period of Ca^{2+} oscillations, i.e., a nonlinear increment of Ras-GTP level is observed with the increase of oscillatory frequency. It should be pointed out that a sharp increase of the average Ras-GTP is displayed when the period of Ca^{2+} oscillations is changed from 120 s to 60 s in the experiment [25] while the average Ras-GTP from our result is still small when the period is about 18.33 s. Our theoretical curve is similar to the experimental observation when the period is beyond 120 s. The monotonous dependence curve can be explained as below. The produce rate of Ras-GTP in Eq. (10) is an increasing function of Ca^{2+} concentration. The average Ca^{2+} concentration gets bigger as the frequency of Ca^{2+} oscillations turns larger. Thus, increasing the frequency of Ca^{2+} oscillations leads to the increase of Ras-GTP. Furthermore, the dependence of maximal Ras-GTP on the period of Ca^{2+} oscillations is given in Fig. 4(b). It is found that the concentration of maximal Ras-GTP is at a high level. A very weak negative correlation between the peak value of Ras-GTP and period of Ca^{2+} oscillations is found.

3.2. Different roles of oscillatory and constant Ca^{2+} signals

Previous model and experimental studies using simple spiking Ca^{2+} oscillations have shown that an oscillatory Ca^{2+} signal can decrease the effective calcium threshold for the activation of an enzyme [41–45], and thus is more efficient, compared with a constant signal. In our model study, we investigate the dependences of average Ras-GTP on the average level of Ca^{2+} signal for oscillatory and constant Ca^{2+} signals, which are shown in Fig. 5. If Ca^{2+} binds cooperatively to the GEF kinase in the GTPase-cycle ($n=2$), a monotonous increasing curve appears as the average Ca^{2+} level increases. Interestingly, in Fig. 5(a), for small average Ca^{2+}, the average Ras-GTP driven by oscillatory Ca^{2+} signal is larger than that driven by constant Ca^{2+}. While for larger average Ca^{2+} level, Ca^{2+} oscillations activate Ras-GTP to a nearly same level as a constant Ca^{2+} signal. This finding is consistent qualitatively with the experimental observation. Our result is still valid for larger cooperativity (data not shown). On the contrary, we find that, in the absence of cooperativity in Ca^{2+} binding to GEF kinase ($n=1$), a constant signal

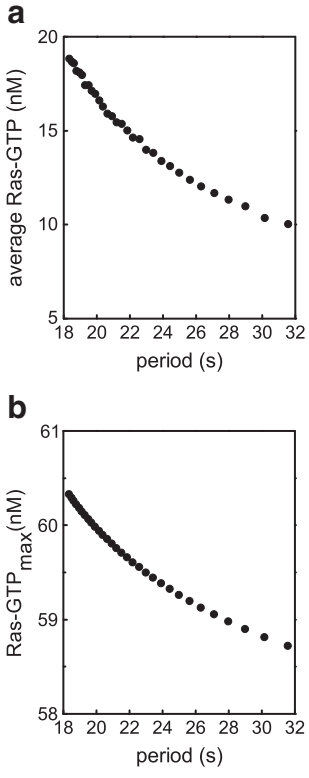

Fig. 4. (a) The average and (b) the maximal Ras-GTP versus the period of Ca^{2+} oscillations.

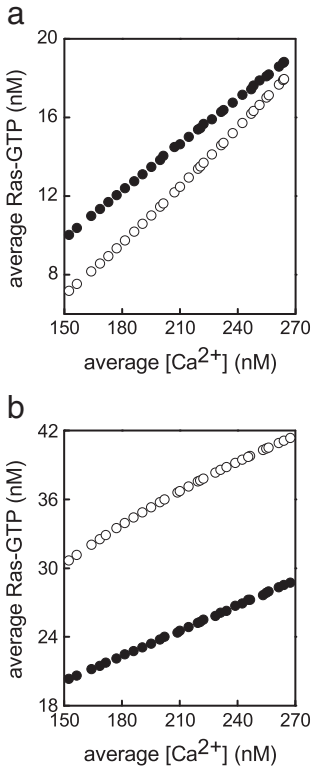

Fig. 5. The comparison of the average Ras-GTP in response to oscillatory (•) and constant (◦) Ca^{2+} signals. (a) $n=2$ for Ca^{2+} binding in GTPase-cycle. (b) The same as (a) for non-cooperative behavior ($n=1$ instead).

is always more efficient in activating Ras-GTP, as shown in Fig. 5(b). This finding is in good agreement with the observation in the experiment [25].

Thus, at the low levels of stimulation, Ca^{2+} oscillations can be more potent in activating Ras than constant Ca^{2+} signal of the same average calcium. However, this requires the binding cooperativity of Ca^{2+} in the GTPase-cycle. The reason is that oscillatory Ca^{2+} signal reduces the effective Ca^{2+} threshold for the activation of Ras compared with the constant Ca^{2+} one. From the above analysis, it clearly shows that the nonlinear interaction might play an important role in this finding.

3.3. Negative correlation between activation of MAPK cascade and period of Ca^{2+} signal when Ca^{2+} oscillations are described by the Li-Rinzel model.

Similar to Ras, the negative correlation between the activation of MAPK cascade and the period of Ca^{2+} oscillations was also observed experimentally (see Fig. 3(b) in Ref. [25]). We use the HOC model to investigate the frequency modulations of Ca^{2+} oscillations on MAPK cascade in the homogeneous system. Here, we define the ratio of average ppMAPK to $[MAPK]_{tot}$ as the activation of MAPK cascade.

The frequency modulations of Ca^{2+} oscillations on activation of MAPK cascade in our HOC model are shown in Fig. 6(a). It is found three kinds of responses, including gradual, step-like and non-monotonic, emerge when MAPK cascade is operated for three different modes. For mode I, the activation shows a gradual decrease as the period of Ca^{2+} signal increases. For mode II, an all-or-none (i.e., binary) response appears due to the positive feedback in the MAPK cascade. The activation switches dramatically from a high level to a very low level when the period of Ca^{2+} oscillations passes through a critical value about 26 s. For mode III, it is observed that the activation is very small during a large range of period, and a non-monotonous stimulus response occurs because of the negative feedback in MAPK cascade. Globally, among three operation modes of MAPK cascade, the activation in mode II is largest among three modes when the period of Ca^{2+} oscillations is smaller than 26 s. After this transition point, the activations of MAPK cascade for all three modes drop to a nearly same low level.

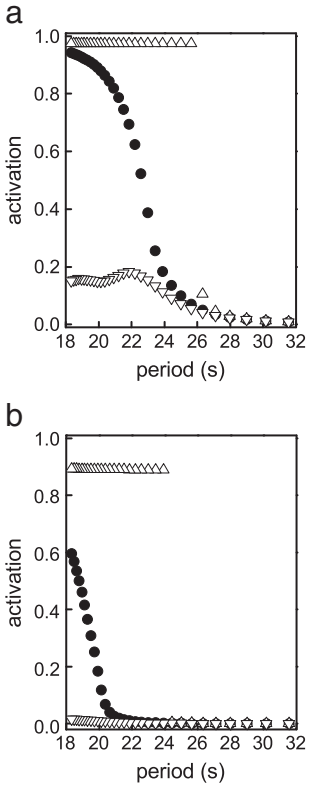

Fig. 6. The activation of MAPK cascade is plotted against the period of Ca^{2+} oscillations for three operation modes (mode I (•), mode II (△), mode III (▽)) in our HOC (left graph) and HEC (right graph) models. Here Ca^{2+} signal is generated by the Li–Rinzel model.

Especially, it is discovered that our numerical result for mode I fits qualitatively with the experimental observation. Two aspects close to the experiment are described. First, a strong negative correlation between the activation and the period of Ca^{2+} oscillations is exhibited. For a very small period of Ca^{2+} oscillations (e.g., 18.33 s), the activation is very large ($activation \approx 0.97$). While the activation of MAPK cascade approaches to zero for a very large period of Ca^{2+} signal. Second, with increasing the period of Ca^{2+} oscillations, the activation decreases gradually, not dramatically. Therefore, our theoretical model is capable of explaining the experimental observation under appropriate conditions. An understanding for the observed negative correlation for mode I is achieved by analyzing the dynamical coordination of GTPase-cycle and MAPK cascade modules. As shown in Fig. 5(a), the average Ras-GTP in the GTPase-cycle is from 10 to 20 nM. During such a region, the MAPK cascade for mode I just undergoes the ultrasensitivity response, as shown in Fig. 3(a). Therefore, with increasing the period of Ca^{2+} oscillations (i.e., decreasing average Ras-GTP), the activation of MAPK cascade is reduced continuously and gradually from a high level to a low level. The dynamic interaction between GTPase-cycle and MAPK cascade leads to this theoretical result. In contrast, the dependence curves for mode II and III both deviate largely from the experiment. Naturally, the appropriate operation mode of MAPK cascade is desirable to achieve the negative correlation.

Above, we have used the HOC model to reveal the negative correlation between the activation of MAPK cascade and the period of Ca^{2+} oscillations in the homogeneous system. Next, we adopt the HEC model to study the responses of activation of MAPK cascade to Ca^{2+} oscillations. It is reported that ppMAPK could be translocated to nucleus and involved in gene regulation network, such as activation of the Xbra transcription factor in Xenopus embryo [46,47]. Thus, we are interested in how the response of ppMAPK at the nucleus to the period of Ca^{2+} oscillations in the heterogeneous system. We define the ratio of average ppMAPK at the nucleus to $[MAPK]_{tot}$ as the activation of MAPK cascade when spatial effects are considered. Below, we investigate the frequency modulations of Ca^{2+} oscillations on activation of MAPK cascade in the heterogeneous system.

As shown in Fig. 6(b), for mode I, a gradual decrease of activation is found by enhancing the period of Ca^{2+} oscillations. We observe a negative correlation between the activation and the period of Ca^{2+} oscillations. The activation of MAPK cascade descends slowly from a high level to a very low level as the period of Ca^{2+} oscillations increases. This result illustrates that our HEC model also provides a fine description for the observed negative correlation behavior. In addition, the response curve drops to zero after passing through a critical period about 22 s. For mode II, a step-like response is found. The response is switched sharply from a high level to a low level when the period of Ca^{2+} oscillations is beyond 24 s. For mode III, the activation is nearly independent on the period of Ca^{2+}. The observations for mode II and III both depart obviously from the experimental finding.

3.4. Negative correlation between activation of MAPK cascade and period of Ca^{2+} signal when Ca^{2+} oscillations are described by a piecewise constant function

It is noted that, due to the inherent dynamical character of the Li–Rinzel model, the frequency-modulation can only lead to Ca^{2+} oscillations with a period changing from 18.33 to 31.55 s, while in the experiment, the period of Ca^{2+} oscillations varies from 60 to 600 s.

The range of period of Ca^{2+} oscillations investigated in the Li–Rinzel model is much smaller than that of the experiment. It would be much more meaningful to generate Ca^{2+} signal in an artificial way to cover the range of period of Ca^{2+} oscillations in Ref. [25].

Cytosolic Ca^{2+} oscillations consist of a series of spikes separated by intervals of resting Ca^{2+} oscillations [48]. Here for simplicity, Ca^{2+} oscillations are described by a piecewise constant function

$$S(t) = \begin{cases} S_0, & iT \le t < iT + \Delta \\ 0 & iT + \Delta \le t < (i+1)T \end{cases} \quad (26)$$
$$i = 0, \cdots, \infty,$$

characterized by period T, amplitude S_0, spike width Δ, and the basal Ca^{2+} oscillation has been set to zero. We use this piecewise constant function instead of the Li–Rinzel model in our study. We also fix $S_0 = 1500$ nM, $\Delta = 20$ s, and let T change from 60 to 600 s. Therefore we can explore all the periods and the average Ca^{2+} concentration as those in the experiment by adjusting the period T, this allows us to compare our theoretical results with experimental findings in the similar level of Ca^{2+} signal.

Using Eq. (26) instead of Eqs. (1) and (2) in our HOC model, we study the dependence of activation of MAPK cascade on the period of Ca^{2+} oscillations. In Fig. 7(a), different from the above case adopting the Li–Rinzel model, all three operation modes can induce the negative correlation between the activation and the period of Ca^{2+} oscillations. Especially, for mode I and II, the activation decreases slowly from a high level (close to 1.0) to a very low level (about 0.1) when the period of Ca^{2+} oscillations increases from 60 to 600 s, fitting well with the experimental observation. The slight differences among three negative correlation curves are due to various feedback mechanisms in MAPK cascade. Our results illustrate that the negative correlation is perhaps an intrinsic phenomenon for the situation if Ca^{2+} signal is modeled by the piecewise constant function. The

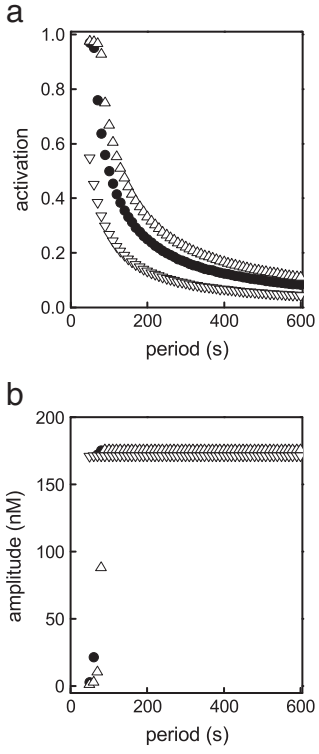

Fig. 7. (a) The activation of MAPK cascade and (b) the amplitude of ppMAPK versus the period of Ca^{2+} oscillations for three operation modes (mode I (•), mode II (△), mode III (▽)) in our HOC model. Here a piecewise constant function is used instead of the Li–Rinzel model.

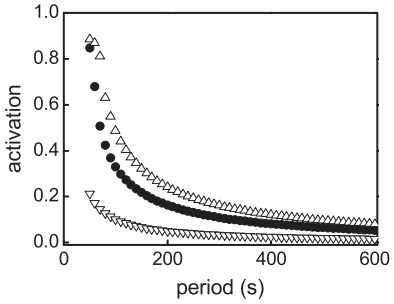

Fig. 8. The activation of MAPK cascade is plotted against the period of Ca^{2+} oscillations for three operation modes (mode I (•), mode II (△), mode III (▽)) in our HEC model. Here a piecewise constant function is used instead of the Li–Rinzel model.

occurrence of negative correlation between the activation of MAPK cascade and the period of Ca^{2+} signal is not dependent on the specific operation mode of MAPK cascade.

In addition, in order to examine whether it is more appropriate to show the amplitudes of ppMAPK oscillations rather than the average, the dependence of amplitude of ppMAPK oscillations on the period of piecewise function for different modes is also explored in Fig. 7(b). It is found that, except for very small period, the amplitude is almost unchanged as the period of Ca^{2+} signal increases. This result shows that the amplitude is not a good measurement for the activation of MAPK cascade.

When we replace Eqs. (1) and (2) by Eq. (26) in the HEC model, we also obtain the dependence of the activation of MAPK cascade on the period of Ca^{2+} oscillations for different modes in the heterogeneous system. As shown in Fig. 8, it is seen that the negative correlation appears for all three modes. Especially, for mode I and II, the activation drops slowly from a high to a low level as increasing the period of Ca^{2+} oscillations, showing strong negative correlation behavior. For mode III, the negative correlation is slightly weak, because the activation under small period of Ca^{2+} signal (e.g., 60 s) is small (about 0.2). In a word, the results in a heterogeneous system highlight that the negative correlation is independent on the operation mode, and the different feedback control in MAPK cascade only modulates the strength of negative correlation.

4. Discussion and conclusion

In summary, motivated by the experimental work [25], the frequency modulations of Ca^{2+} signal on activation of Ras and MAPK cascade are studied by theoretical modeling and numerical analysis. For the homogeneous system, an integrated theoretical model is built to couple Ca^{2+} oscillations, GTPase-cycle and MAPK cascade modules in sequence. Meanwhile, based on different types of feedback in MAPK cascade, three operation modes of this model are introduced. Then an extended theoretical model, i.e., a reaction–diffusion model is built when the spatial effects are involved in the heterogeneous system. Using these two models, we investigate systematically the frequency modulations of Ca^{2+} signal on activation of MAPK cascade under both the homogeneous and heterogeneous conditions. (i) When the Li–Rinzel model is adopted to generate Ca^{2+} oscillations, we find that there exists a negative correlation between a decreasing frequency of Ca^{2+} oscillations and average Ras-GTP concentration, and Ras-GTP can be more efficiently activated by an oscillatory Ca^{2+} signal than a constant signal if Ca^{2+} acts cooperatively on the GEF kinase. Furthermore, we identify that the operation mode of MAPK cascade plays crucial role in reproducing the negative correlation between activation of MAPK cascade and period of Ca^{2+} oscillations. (ii) Moreover, when a piecewise function is used instead of the Li–Rinzel model to cover the range of periods of Ca^{2+} signal in the experiment, we observe that the negative correlation feature is

independent on the operation mode of MAPK cascade, and the feedback regulations in MAPK cascade only influence the strength of negative correlation. In this case, perhaps, there is no need to go back to the nonlinear engineering or mathematics literature to achieve this negative correlation behavior.

The modeling approach employed here has a number of limitations. First, to build a complete model describing the real biological process of Ca^{2+}-mediated MAPK signaling pathway is not easy. The Li–Rinzel model of Ca^{2+} oscillations (or a piecewise constant function) and a three-layer MAPK cascade model are coupled by a simplified GTPase-cycle module in our theoretical models. It is worth mentioning that the Ca^{2+}-dependent activation of Ras through GEF is modeled by Michaelis–Menten kinetics, some intermediate proteins are neglected in this process. The hypothesis that the deactivation of Ras is assumed to be independent on GAP concentration may be a little simple. Second, some parameter values for reaction rates are chosen from previous literatures, however some unknown parameter values are presented empirically. Whether our results found here are affected by the change in parameters should be examined in a broader parameter space by random parameter search [49]. Third, here we only consider Ca^{2+} oscillations described by a limit cycle or a piecewise constant function, we do not include the stochastic origin in Ca^{2+} dynamics [50,51]. To analyze the stochastic and transient behavior in Ca^{2+} oscillations even the Ca^{2+}-mediated MAPK signaling pathway will also be an interesting problem [52,53].

Our work suggests that the appropriate combination of three modules leads to the biological function of Ca^{2+}-mediated MAPK signaling pathway and reproduces the experimental findings. These findings enrich our understanding of the mechanism of negative correlation between the activation of MAPK cascade and the period of Ca^{2+} oscillations. Our work also provides insights into the relationship between complicated network and fundamental function modules, and gives possible experimental clues for future research.

Acknowledgments

This work was supported by the National Natural Science Foundation of China under Grant No.10905089 (MY), TianYuan Special Funds under Grant No.10926065 (MY), Fundamental Research Funds for the Central Universities of China under Grant Nos. 2010QNA36 (JT), and Natural Science Foundation of China under Grant No.11047146 (CJW), Natural Science Foundation of Shanxi province of China under Grant No.2010JQ1014 (CJW). We are grateful to acknowledge Dr. De Pittà for helpful discussions about Fig. 2.

Appendix A. Supplementary data

Supplementary data to this article can be found online at doi:10.1016/j.bpc.2011.04.007.

References

[1] W. Kolch, Coordinating ERK/MAPK signalling through scaffolds and inhibitors, Nat. Rev. Mol. Cell Biol. 6 (2005) 827–837.
[2] M. Raman, W. Chen, M.H. Cobb, Differential regulation and properties of MAPKs, Oncogene 26 (2007) 3100–3112.
[3] M.J. Berridge, M.D. Bootman, H.L. Roderick, Calcium signalling: dynamics, homeostasis and remodelling, Nat. Rev. Mol. Cell Biol. 4 (2003) 517–529.
[4] M.J. Berridge, P. Lipp, M.D. Bootman, The versatility and universality of calcium signalling, Nat. Rev. Mol. Cell Biol. 1 (2000) 11–21.
[5] A. Politi, L.D. Gaspers, A.P. Thomas, T. Höfer, Models of IP_3 and Ca^{2+} oscillations: frequency encoding and identification of underlying feedbacks, Biophys. J. 90 (2006) 3120–3133.
[6] U. Kummer, L.F. Olsen, C.J. Dixon, A.K. Green, E. Bomberg, G. Baier, Switching from simple to complex oscillations in calcium signaling, Biophys. J. 79 (2000) 1188–1195.
[7] M.S. Nash, K.W. Young, R.A.J. Chaliss, S.R. Nahorski, Intracellular signalling: receptor-specific messenger oscillations, Nature 413 (2001) 381–382.
[8] M.D. Bootman, P. Lipp, M.J. Berridge, The organisation and functions of local Ca^{2+} signals, J. Cell Sci. 114 (2001) 2213–2222.
[9] G. Dupont, A. Goldbeter, Protein phosphorylation driven by intracellular calcium oscillations: a kinetic analysis, Biophys. Chem. 42 (1992) 257–270.
[10] F.H. Cruzalegui, H. Bading, Calcium-regulated protein kinase cascades and their transcription factor targets, Cell. Mol. Life Sci. 57 (2000) 402–410.
[11] C.L. Zhu, Y. Zheng, Y. Jia, A theoretical study on activation of transcription factor modulated by intracellular Ca^{2+} oscillations, Biophys. Chem. 129 (2007) 49–55.
[12] L. Chang, M. Karin, Mammalian MAP kinase signalling cascades, Nature 410 (2001) 37–40.
[13] M. Qi, E.A. Elion, MAP kinase pathways, J. Cell Sci. 118 (2005) 3569–3572.
[14] B.N. Kholodenko, Spatially distributed cell signalling, FEBS Lett. 583 (2009) 4006–4012.
[15] B.N. Kholodenko, M.R. Birtwistle, Four-dimensional dynamics of MAPK information processing systems, Wiley Interdiscip. Rev. Syst. Biol. Med. 1 (2009) 28–44.
[16] B.N. Kholodenko, J.F. Hancock, W. Kolch, Signalling ballet in space and time, Nat. Rev. Mol. Cell Biol. 11 (2010) 414–426.
[17] A. Fujioka, K. Terai, R.E. Itoh, K. Aoki, T. Nakamura, S. Kuroda, E. Nishida, M. Matsuda, Dynamics of the Ras/ERK MAPK cascade as monitored by fluorescent probes, J. Biol. Chem. 281 (2006) 8917–8926.
[18] L.O. Murphy, S. Smith, R.H. Chen, D.C. Fingar, J. Blenis, Molecular interpretation of ERK signal duration by immediate early gene products, Nat. Cell Biol. 4 (2002) 556–564.
[19] P.J. Cullen, P.J. Lockyer, Integration of calcium and RAS signalling, Nat. Rev. Mol. Cell Biol. 3 (2002) 339–348.
[20] S.A. Walker, P.J. Lockyer, P.J. Cullen, The Ras binary switch: an ideal processor for decoding complex Ca^{2+} signals? Biochem. Soc. Trans. 31 (2003) 966–969.
[21] L.B. Rosen, D.D. Ginty, M.J. Weber, M.E. Greenberg, Membrane depolarization and Ca^{2+} influx stimulate MEK and MAP kinase via activation of Ras, Neuron 12 (1994) 1207–1221.
[22] P. Marambaud, U. Dreses-Werringloer, V. Vingtdeux, Calcium signaling in neurodegeneration, Mol. Neurodegener. 4 (2009) 20–34.
[23] J.D. Sweatt, Mitogen-activated protein kinases in synaptic plasticity and memory, Curr. Opin. Neurobiol. 14 (2004) 311–317.
[24] G.M. Thomas, R.L. Huganir, MAPK cascade signalling and synaptic plasticity, Nat. Rev. Neurosci. 5 (2004) 173–183.
[25] S. Kupzig, S.A. Walker, P.J. Cullen, The frequencies of calcium oscillations are optimized for efficient calcium-mediated activation of Ras and the ERK/MAPK cascade, Proc. Natl. Acad. Sci. U. S. A. 102 (2005) 7577–7582.
[26] J. Díaz, G. Baiera, G. Martínez-Meklerb, N. Pastor, Interaction of the IP_3-Ca^{2+} and the FGF-MAPK signaling pathways in the *Xenopus laevis* embryo: a qualitative approach to the mesodermal induction problem, Biophys. Chem. 97 (2002) 55–72.
[27] Q. Zhao, M. Yi, K. Xia, M. Zhan, Information propagation from IP_3 to target protein: a combined model for encoding and decoding of Ca^{2+} signal, Physica A 388 (2009) 4105–4114.
[28] Y.X. Li, J. Rinzel, Equations for $InsP_3$ receptor-mediated $[Ca^{2+}]_i$ oscillations derived from a detailed kinetic model: a Hodgkin–Huxley like formalism, J. Theor. Biol. 166 (1994) 461–473.
[29] M.J. Berridge, The AM and FM of calcium signalling, Nature 389 (1997) 759–760.
[30] M. De Pittà, V. Volman, H. Levine, G. Pioggia, D. De Rossi, E. Ben-Jacob, Coexistence of amplitude and frequency modulations in intracellular calcium dynamics, Phys. Rev. E 77 (2008) 030903-1-4.
[31] C.Y. Huang, J.E. Ferrell, Ultrasensitivity in the mitogen-activated protein kinase cascade, Proc. Natl. Acad. Sci. U. S. A. 93 (1996) 10078–10083.
[32] B.N. Kholodenko, Negative feedback and ultrasensitivity can bring about oscillations in the mitogen-activated protein kinase cascades, Eur. J. Biochem. 267 (2000) 1583–1588.
[33] N.I. Markevich, M.A. Tsyganov, J.B. Hoek, B.N. Kholodenko, Long-range signaling by phosphoprotein waves arising from bistability in protein kinase cascades, Mol. Syst. Biol. 2 (2006) 61.
[34] R. Heinrich, B.G. Neel, T.A. Rapoport, Mathematical models of protein kinase signal transduction, Mol. Cell 9 (2002) 957–970.
[35] J.E. Ferrell, How responses get more switch-like as you move down a protein kinase cascade, Trends Biochem. Sci. 22 (1997) 288–289.
[36] G.C. Brown, J.B. Hoek, B.N. Kholodenko, Why do protein kinase cascades have more than one level, Trends Biochem. Sci. 22 (1997) 288.
[37] U.S. Bhalla, P.T. Ram, R. Iyengar, MAP kinase phosphatase as a locus of flexibility in a mitogen-activated protein kinase signaling network, Science 297 (2002) 1018–1023.
[38] N.I. Markevich, J.B. Hoek, B.N. Kholodenko, Signaling switches and bistability arising from multisite phosphorylation in protein kinase cascades, J. Cell Biol. 164 (2004) 353–359.
[39] Q. Zhao, M. Yi, Y. Liu, Spatial distribution and dose-response relationship for different operation modes in a reaction-diffusion model of MAPK cascade, Phys. Biol. (forthcoming) http://iopscience.iop.org/1478-3975/page/Forthcoming%20articles#Special_isq-bio.
[40] G.C. Brown, B.N. Kholodenko, Spatial gradients of cellular phospho-proteins, FEBS Lett. 457 (1999) 452–454.
[41] C. Salazar, A.Z. Politi, T. Höfer, Decoding of calcium oscillations by phosphorylation cycles: analytic results, Biophys. J. 94 (2008) 1203–1215.
[42] R.E. Dolmetsch, E. Xu, R.S. Lewis, Calcium oscillations increase the efficiency and specificity of gene expression, Nature 392 (1998) 933–936.
[43] W.H. Li, J. Llopis, M. Whitney, G. Zlokarnik, R. Tsien, Cell-permeant caged $InsP_3$ ester shows that Ca^{2+} spike frequency can optimize gene expression, Nature 392 (1998) 936–941.
[44] L.T. Izu, R.A. Spangler, A class of parametrically excited calcium oscillation detectors, Biophys. J. 68 (1995) 1621–1629.
[45] D. Gall, E. Baus, G. Dupont, Activation of the liver glycogen phosphorylase by Ca^{2+} oscillations: a theoretical study, J. Theor. Biol. 207 (2000) 445–454.

[46] K.L. Curran, R.M. Grainger, Expression of activated MAP kinase in *Xenopus laevis* embryos: evaluating the roles of FGF and other signaling pathways in early induction and patterning, Dev. Biol. 228 (2000) 41–56.
[47] J. Díaz, G. Martínez-Mekler, Interaction of IP_3-Ca^{2+} and MAPK signaling systems in the Xenopus blastomere: a possible frequency encoding mechanism for the control of the Xbra gene expression, Bull. Math. Biol. 67 (2005) 433–465.
[48] A.P. Thomas, G.S. Bird, G. Hajnoczky, L.D. Robb-Gaspers, J.W. Putney Jr., Spatial and temporal aspects of cellular calcium signaling, FASEB J. 10 (1996) 1505–1507.
[49] L. Qiao, R.B. Nachbar, I.G. Kevrekidis, S.Y. Shvartsman, Bistability and oscillations in the Huang–Ferrell model of MAPK signaling, PLoS Comput. Biol. 9 (3) (2007) 1819–1826.
[50] M. Falcke, L. Tsimring, H. Levine, Stochastic spreading of intracellular Ca^{2+} release, Phys. Rev. E 62 (2000) 2636–2643.
[51] M. Falcke, On the role of stochastic channel behavior in intracellular Ca^{2+} dynamics, Biophys. J. 84 (2003) 42–56.
[52] M. Yi, K. Xia, M. Zhan, Theoretical study for regulatory property of scaffold protein on MAPK cascade: a qualitative modeling, Biophys. Chem. 147 (2010) 130–139.
[53] M. Yi, Q. Liu, Michaelis–Menten mechanism for single-enzyme and multi-enzyme system under stochastic noise and spatial diffusion, Physica A 389 (2010) 3791–3803.